# Wolf effect of partially coherent light fields in two-dimensional curved space

Chenni Xu, Adeel Abbas, Li-Gang Wang,* and Shi-Yao Zhu
*Department of Physics, Zhejiang University, Hangzhou 310027, China*

M. Suhail Zubairy
*Institute for Quantum Science and Engineering (IQSE) and Department of Physics and Astronomy, Texas A&M University, College Station, Texas 77843-4242, USA*

(Received 12 March 2018; published 13 June 2018)

Wolf effect refers to a spectral shift of light during its propagation even in free space, which results from the fluctuating (or correlation) nature of light sources. In conventional optics, the propagation laws of light are usually considered in flat space. However, optical phenomena are fascinating in the presence of space curvature. Here the problem of spectral changes of light during its propagation is addressed in a two-dimensional (2D) curved space, and the influence of space curvature on the Wolf effect is revealed. The propagation expression for a partially coherent polychromatic light beam is analytically derived for propagating inside 2D curved surfaces of revolution with constant Gaussian curvature under a linear paraxial approximation. It shows that the curved spaces with larger positive curvature accelerate and enhance the spectral shifts (blue- and redshifts) of light during their propagation, and the spaces with larger negative curvature may decelerate and suppress the spectral shifts. Furthermore, different correlation lengths of light sources also affect the behaviors of spectral shifts of light in such curved surfaces of revolution. Our result provides a method to measure the curvature of curved space by measuring the spectral shift of light during its propagation in curved space, like the cases of light propagating in practical gravitational space.

DOI: 10.1103/PhysRevA.97.063827

## I. INTRODUCTION

Spectroscopy of light radiation is one of the most important methods in science and technology, and it has become a very powerful tool in many applications such as the characterization of the properties of light sources, the energy-level structures of atomic and molecular particles, and the absorption and emission features from material media and/or biological units. However, the spectrum of light radiation emitted by an object can change on propagation to the observer even when it travels through empty space. Currently, there are several well-known mechanisms which can lead to the change of light spectrum. For example, it is well known that due to the Doppler effect, the spectrum of light suffers red- or blueshifts for an observer who moves relatively away from or toward the source. The spectral change also occurs in the electromagnetic emission of surface systems in the near and the far zones because of the loss of evanescent modes on propagation [1].

Here we want to address another important effect on spectral change whose origin lies in the fluctuating (statistical) nature of the light sources [2,3]. This kind of spectral change due to the correlation of the light source is sometimes termed as correlation-induced spectral change (see a review in Ref. [4]), and it is also called the Wolf effect [5–7]. The spectral change caused by the Wolf effect has been verified in several experimental systems, such as ordinary partially coherent light sources [8,9], acoustic-correlated systems [10,11], diffraction of light through an aperture system [12,13], thermal-emitted spectra of the infrared source from a periodic microstructure with polar materials [7], and the propagation of light in biological tissues [14]. The Wolf effect has also been theoretically extended to study both the spectral changes of light from scattering systems [15] and the application to inverse scattering problems [16]. Although the theories and applications of partially coherent sources have attracted much attention [17–24], studies on the Wolf effect recognized as an intriguing phenomenon of partially coherent sources are all limited to simple optical systems in flat space. In this work, we are going to investigate the Wolf effect of light propagating on a special two-dimensional (2D) curved space whose curvature effect may lead to the extraordinary spectral change of light.

Up to now, the physics of curved space-time predicted by general relativity is still hard to be accessed directly in laboratory experiments; however, researchers have suggested various physical systems theoretically or experimentally to demonstrate the analogous effects in curved space-time [25–46]. For instance, it is possible to simulate the black-hole evaporation and Hawking emission from the black-hole analogs in a flowing fluid [25–27], and it is also known to create a sonic horizon, Gibbons-Hawking effect, and a sonic black-hole analog in Bose-Einstein condensed systems [28–31]. More interestingly, optical and electromagnetic analogs of curved spaces like gravitational fields and lenses have been demonstrated in moving dielectric media [32–34], designed electromagnetic waveguides [37–39], microstructured optical fibers [41], nonlinear Newton-Schrödinger systems [43,44], and metamaterial systems [45,46]. All these

*sxwlg@yahoo.com

 

studies show that optical analogs are excellent table-top candidates for studying gravitational phenomena.

Another route is to directly fabricate the geometry of a curved space-time and investigate the consequence of space-time curvature on light propagations with reduced dimensionality (i.e., one-dimensional (1D) curved lines or 2D curved surfaces). As a matter of fact, studies of physics on curved surfaces can trace back to the middle and late twentieth century from two seminal works [47,48]. Now it is commonly accepted that a curved surface offers a curvature-induced geometrical potential which therefore influences the dynamics of particles, electronic states, and fields. In the recent decade, there have been an increasing number of interesting investigations on light propagation in curved space [49–59], which are seen as direct platforms to reveal the interplay effects between light and curved space-time and promote the understanding of the general-relativity concepts with light propagations. Light propagations in 2D curved space can be achieved by covering a thin film served as waveguide on a three-dimensional object or by total internal reflection. An effective theory describing the propagation of light on a general curved surface has been developed and the properties of linear propagation of an initially Gaussian profile on surfaces of revolution with constant Gaussian curvature were first investigated in Ref. [49], and has since been experimentally demonstrated on a sphere and a hyperbolic surface [50]. One can also find the solutions for shape-preserving spatially accelerating wave packets in curved space where accelerating wave packets may propagate along nongeodesic trajectories [53], and such behaviors have been experimentally observed [54]. In addition, topological phases in curved-space photonic lattices have been introduced, which may lead to curvature-induced topological edge states and topological phase transitions [55]. Very recently, the Hanbury-Brown–Twiss effect was revisited in the presence of space curvature [57], and it was shown that the evolution of speckle patterns is very distinct in 2D surfaces of constant positive and negative Gaussian curvature and the surfaces with constant Gaussian curvature act as analog models for universes having nonvanishing cosmological constants [57].

It is well known that in astronomy the redshift of light from distant galaxies also happens due to the expansion of space, and such a redshift is known as a cosmological redshift derived from the Robertson-Walker metric under the formalism of general relativity [60]. Although the spectral change caused by the Wolf effect was seen as a noncosmological redshift which may be responsible for inexplicable astronomical phenomena such as observed spectral redshift of certain extragalactic celestial bodies like quasars [6,61], it would be very physically meaningful to consider the Wolf effect in the presence of space curvature. Special types of surfaces can be emulated as a uniform and isotropic universe because of translational and rotational symmetry. In this work, the gravitational effect is embodied in the shape of the surface, i.e., the distribution of curvature, and a gravitational source is not necessarily included, therefore the nonlinear process is not considered. Here we reveal the influence of the curved space on the spectral shift of a partially coherent polychromatic light propagating along such surfaces of revolutions with positive or negative constant Gaussian curvature.

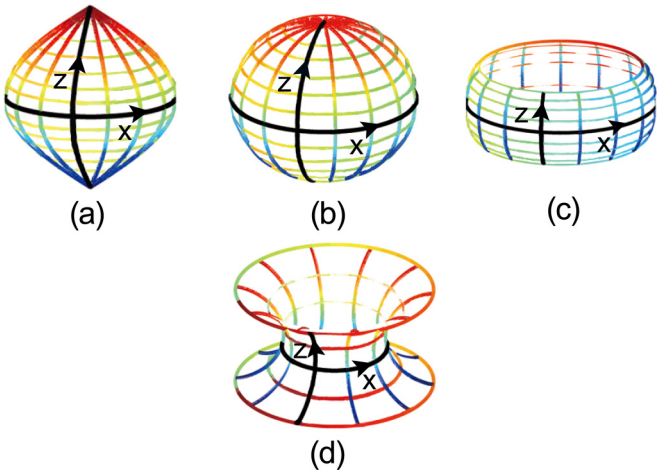


FIG. 1. Surfaces of revolution with constant positive (a)–(c) and negative (d) curvature. For positive curvature, different relations between radius of curvature $R$ and the constant $R_0$ lead to three types of surfaces: (a) spindle with $R_0 < R$, (b) sphere with $R_0 = R$, and (c) bulge with $R_0 > R$. While for negative curvature, there is only the hyperboloid type of surface in our case. The curvilinear coordinate on the surface defined in this work is also illustrated, where the propagating axis of light is $z$ and the proper length in the transverse direction on the surface is $x$. Here we should note that on the initial plane of $z = 0$, $x$ is equal to coordinate $\xi$ during the calculation, and $\eta$ at $z > 0$ is not $x$ any more.

## II. BRIEF REVIEW ON SURFACES OF REVOLUTION

First we briefly introduce a type of 2D curved spaces: surfaces of revolution. For convenience of parametrization, the profile curve of such 2D curved surfaces of revolution can be expressed by the vector $\mathbf{s} = [r(z)\cos\varphi, r(z)\sin\varphi, h(z)]$ in Cartesian coordinates [57], where the parameter $z$ is the proper length along the profile curve, thus $(dr(z)/dz)^2 + (dh(z)/dz)^2 = 1$ is always satisfied. Once the radius parametrization $r(z)$ is known, such surfaces are determined. For a surface of revolution with Gaussian curvature, its intrinsic curvature is defined as $K = \kappa_1\kappa_2$, where $\kappa_{1,2} = 1/R_{1,2}$ are principal curvatures related to those two tangent circles with maximal and minimal radii $R_1$ and $R_2$ for every regular point on the surface. The parameter $K$ is merely determined by the metric $g_{ij}$ of the surface and is not related to its topological shape, and it can even be negative when tangent circles locate at opposite sides of the surface. It should be mentioned that such surfaces of revolution always obey the differential equation $dr^2(z)/d^2z + Kr(z) = 0$, which can also give the value of $K$ for a given function $r(z)$.

As in Refs. [49,50,57], we consider the surfaces of revolution parametrized by $r(z) = R_0\cos_q(z/R)$, where $q = \mathrm{sgn}(K)$, and $R_0$ is an arbitrary positive constant which scarcely influences physical properties but decides the shape of the surface (see Fig. 1). We define these functions $\sin_q(a)$, $\cos_q(a)$, and $\tan_q(a)$ to be $\sin(a)$, $\cos(a)$, and $\tan(a)$ for $q = +1$ and to be $\sinh(a)$, $\cosh(a)$, and $\tanh(a)$ for $q = -1$. Clearly, in this situation the Gaussian curvature is a constant given by $K = 1/R^2$ for $q = +1$ or $K = -1/R^2$ for $q = -1$. For constant $K > 0$, when $R = R_0$, it is a spherical surface; when $R > R_0$, it is a spindle-type surface; when $R < R_0$, it becomes

the bulge type. Since the value of $r(z)$ should be positive, the range of $z$ should be $(-\pi R/2,\pi R/2)$ for $R \geqslant R_0$ or $(-R\arcsin(R/R_0), R\arcsin(R/R_0))$ for $R < R_0$. For $K < 0$, we have $|z| < R\ \mathrm{arcsin\,h}(R/R_0)$. With $\xi = R_0\varphi$, we get the following metric:

$$ds^2 = dz^2 + \cos_q^2(z/R)d\xi^2, \tag{1}$$

with $\xi \in [-\pi R_0,\pi R_0)$. Therefore the covariant Laplace operator is given by [49]

$$\Delta = \partial_z^2 - \frac{q}{R}\tan_q(z/R)\partial_z + \cos_q^{-2}(z/R)\partial_\xi^2. \tag{2}$$

Therefore we obtain the Helmholtz equation of light in 2D curved space.

## III. PROPAGATION OF LIGHT IN 2D CURVED SPACE

We consider the propagation of a partially coherent polychromatic light beam inside a 2D curved surface. As shown in Fig. 1, the light propagates along the longitudinal direction $z$ on surfaces from the initial plane $z = 0$ to an arbitrary plane $z > 0$. In this work, we only discuss the rotationally symmetric macroscopic case when the wave number of light is significantly large compared to the curvature $K$. The effect of the extrinsic (or mean) curvature $H$ related to the topology is negligible because light cannot distinguish local surroundings [50]. Using the above covariant Laplace operator and the Helmholtz equation, for a 2D curved surface with constant $K$, the point spread function (or Green's function) of light, from the source plane $\xi$ at $z = 0$ to arbitrary plane $\eta$ at $z > 0$ in the paraxial approximation, can be derived and it is given by [57]

$$h_q(\xi,\eta,z) = f(z)\left[\frac{k_{\mathrm{eff}}}{2\pi i R\sin_q(z/R)}\right]^{1/2} e^{\frac{ik_{\mathrm{eff}}(\xi-\eta)^2}{2R\tan_q(z/R)}}, \tag{3}$$

where $k_{\mathrm{eff}} = \omega n_{\mathrm{eff}}/c$ is the effective wave number with the effective refractive index $n_{\mathrm{eff}}$ in such curved surfaces, $c$ is the speed of light in vacuum, $f(z) = \exp\left[ik_{\mathrm{eff}}z + \frac{i}{2k_{\mathrm{eff}}}\int_0^z V_{\mathrm{eff},q}(z')\,dz'\right]$, and $V_{\mathrm{eff},q} = q[1+\cos_q^{-2}(z/R)]/(4R^2)$ is the effective potential caused by the curved space and it only depends on $z$. Here we denote $\xi$ as $\eta$ for the plane of $z > 0$. As for nonparaxial case, i.e., when the divergence angle is large or the beam width is comparable with wavelength, unfortunately, Eq. (3) is no longer valid. However, although paraxial approximation is strictly satisfied in this work and discussion will consequently focus on the paraxial case, nonparaxial propagation in curved space is an intriguing problem which is worth further exploration. With the knowledge of the point spread function $h_q(\xi,\eta,z)$ and the theory of coherence, the output cross-spectral density from the correlated source at $z = 0$ to arbitrary position $z$ can be expressed by [62]

$$\begin{aligned} W_{\mathrm{out}}(\eta_1,\eta_2,z,\omega) &= \langle E_{\mathrm{out}}(\eta_1,z,\omega)E^*_{\mathrm{out}}(\eta_2,z,\omega)\rangle \\ &= \iint W_{\mathrm{in}}(\xi_1,\xi_2,0,\omega)h_q(\xi_1,\eta_1,z) \\ &\quad\times h_q^*(\xi_2,\eta_2,z)d\xi_1 d\xi_2, \end{aligned} \tag{4}$$

where $W_{\mathrm{in}}(\xi_1,\xi_2,0,\omega)$ is the initial cross-spectral density of the source, and $\xi_{1,2}$ and $\eta_{1,2}$ are the transverse coordinates at $z = 0$ and $z > 0$, respectively. Here the proper length in the $\xi$ or $\eta$ direction is $x = \xi\cos_q(z/R)$ or $x = \eta\cos_q(z/R)$. We assume the spot size $\sigma_s$ of the initial light source is extremely smaller than the value of $|\pi R_0|$ for a well-collimated narrow beam, i.e., $\sigma_s \ll |\pi R_0|$, then the integral interval can be mathematically expanded into the range of $(-\infty, +\infty)$. For simplicity but without loss of generality, the initial cross-spectral density of the partially coherent polychromatic light source here is described by a Gaussian Schell-model with a single spectral peak. Thus $W_{\mathrm{in}}(\xi_1,\xi_2,0,\omega)$ for such a light source can be expressed as [3,63]

$$W_{\mathrm{in}}(\xi_1,\xi_2,0,\omega) = S_0(\omega)e^{-\frac{\xi_1^2+\xi_2^2}{4\sigma_s^2}}e^{-\frac{(\xi_1-\xi_2)^2}{2\sigma_g^2}}, \tag{5}$$

where $\sigma_s$ and $\sigma_g$ are the beam half-width and spectral coherence width of the source, respectively, and $S_0(\omega)$ is the initial spectrum of light. Substituting Eq. (5) into Eq. (4), we can analytically derive the output cross-spectral density as

$$\begin{aligned} &W_{\mathrm{out}}(x_1,x_2,z,\omega) \\ &= \frac{S_0(\omega)}{\Omega_q(z,\omega)}\exp\left[-\frac{(x_1^2+x_2^2)}{4\sigma_s^2\Omega_q^2(z,\omega)}\right] \\ &\quad\times\exp\left[-\frac{(x_1-x_2)^2}{2\sigma_g^2\Omega_q^2(z,\omega)} + \frac{ik_{\mathrm{eff}}(x_1^2-x_2^2)}{2\Phi(z,\omega)}\right], \end{aligned} \tag{6}$$

where

$$\Omega_q(z,\omega) = \left[\cos_q^2(z/R) + R^2\sin_q^2(z/R)/Z_R^2(\omega)\right]^{1/2} \tag{7}$$

is the beam-expansion coefficient in such curved surfaces, the function $\Phi(z,\omega) = Z_R^2(\omega)\Omega_q^2(z,\omega)/[R\tan_q(z/R)]$ is related to the radius of curvature of such a partially coherent polychromatic light beam in curved spaces, and $Z_R(\omega) = 2k_{\mathrm{eff}}\sigma_s^2/[1+4\sigma_s^2/\sigma_g^2]^{1/2}$ is the frequency-dependent Rayleigh distance of the initial beam. When $R \to \infty$, the above results will tend to be the same as those in the flat space [64]. In the above calculation, we have already replaced the transverse coordinates $\eta_{1,2}$ with the proper lengths $x_{1,2}$.

From Eq. (6), we obtain the output spectrum as follows:

$$\begin{aligned} S(x,z,\omega) &\equiv W_{\mathrm{out}}(x,x,z,\omega) \\ &= \frac{S_0(\omega)}{\Omega_q(z,\omega)}\exp\left[-\frac{x^2}{2\sigma_s^2\Omega_q^2(z,\omega)}\right]. \end{aligned} \tag{8}$$

Since the quantity $\Omega_q(z,\omega)$ is a function of frequency and it also depends on both the curvature $K$ of curved surfaces and the parameters of light beams, it is clearly expected that the resulting spectrum is affected by all these factors.

## IV. RESULTS AND DISCUSSION

In the following discussion, we assume the initial spectrum has only a single spectral line with a Gaussian profile [3,4],

$$S_0(\omega) = \frac{1}{\delta\sqrt{2\pi}}\exp[-(\omega-\omega_0)^2/(2\delta^2)], \tag{9}$$

where $\omega_0$ is the central angular frequency, and $\delta$ is the effective half-width of the spectral line with $\delta < \omega_0$ in our consideration. For better explanations on the spectral shifts, we define the relative shift of the spectral line as $\alpha = (\omega_1 - \omega_0)/\omega_0$, where

$\omega_1$ is the new peak frequency of the propagated spectrum at an observation point. Below, we take the parameters as follows: $\omega_0/2\pi = 500$ THz, and $\delta/\omega_0 = 0.1$. Our results can also be extended to the cases for other types of spectral profiles like a Lorentzian line.

In Fig. 2, we plot the typical effect of the curvature $K$ on the light spectral shifts in such 2D surfaces of revolution at different observation points. From Fig. 2(a), it is evident that at the on-axis observation point ($x = 0$), all the spectral shifts move to the higher frequencies and they increase as $|K|$ increases in the cases of $K > 0$; while the spectral shifts decrease as $|K|$ increases in the cases of $K < 0$, although they are still positive (i.e., blueshifts). In the inset of Fig. 2(a), on the propagating axis, it is seen that the light spectrum in the curved space with positive $K$ has a larger blueshift than the case in the flat (free) space, while the spectrum of light in the curved space with negative $K$ suffers a suppressed blueshift compared with the case of the flat space. In Fig. 2(b), when the observation point is at $x = 1$ mm (which is slightly away from the propagating axis), we also see that in the cases of $K > 0$, the spectral shift may change from the blue- to redshifts as $|K|$ increases; while it may move to the larger blueshift and then decrease in the cases of $K < 0$. When the observation point is at $x = 3$ mm (which is farther away from the propagating axis), see Fig. 2(c), as $|K|$ increases, we find that the spectral shift is toward the lower frequencies (the redshifts) in the cases of $K > 0$, while in the cases of $K < 0$, the spectral redshift gradually reduces and may even become the blueshift. The insets of Figs. 2(b) and 2(c) demonstrate spectral changes in different situations compared with the results of the flat space and the corresponding initial cases. Clearly the curvature of space does influence the spectral shifts of light as it propagates in curved space.

Compared with the result of $K = 0$ (i.e., the flat space), at on-axis observation points, it is found that the curved spaces with larger positive Gaussian curvatures $K$ lead to larger blueshifts, while the curved spaces with larger negative Gaussian curvatures $K$ lead to smaller blueshifts. When the observation point moves away from the propagating axis, the spaces with larger positive $K$ lead to larger redshifts, while the spaces with larger negative $K$ result in smaller redshifts. These properties are demonstrated in Fig. 3. From Fig. 3, we can conclude that, compared with the results in the flat space, the 2D spaces with large positive $K$ accelerate and enhance the spectral shifts from the blue- to redshifts along the transverse coordinates, while the 2D spaces with large negative $K$ decelerate and reduce the spectral shifts from blue- to redshifts along the transverse coordinates.

To explain the above dependence of the spectral shifts on the curvatures of surfaces and the observation points, we further derive the peak frequency $\omega_1$ of the light spectrum at a certain observation point. Since the initial spectrum is assumed to have only one single peak located at $\omega_0$, the new peak frequency $\omega_1$ must obey $\partial S(x,z,\omega)/\partial\omega|_{\omega=\omega_1} = 0$. In general, the relation between $\omega_1$ and the spatial coordinates $(x,z)$ should satisfy the equality as follows:

$$S_0'(\omega_1) + S_0(\omega_1)\left[\frac{x^2}{\sigma_s^2}\frac{1}{\Omega_q^2(z,\omega_1)} - 1\right]\frac{\Omega_q'(z,\omega_1)}{\Omega_q(z,\omega_1)} = 0, \quad (10)$$

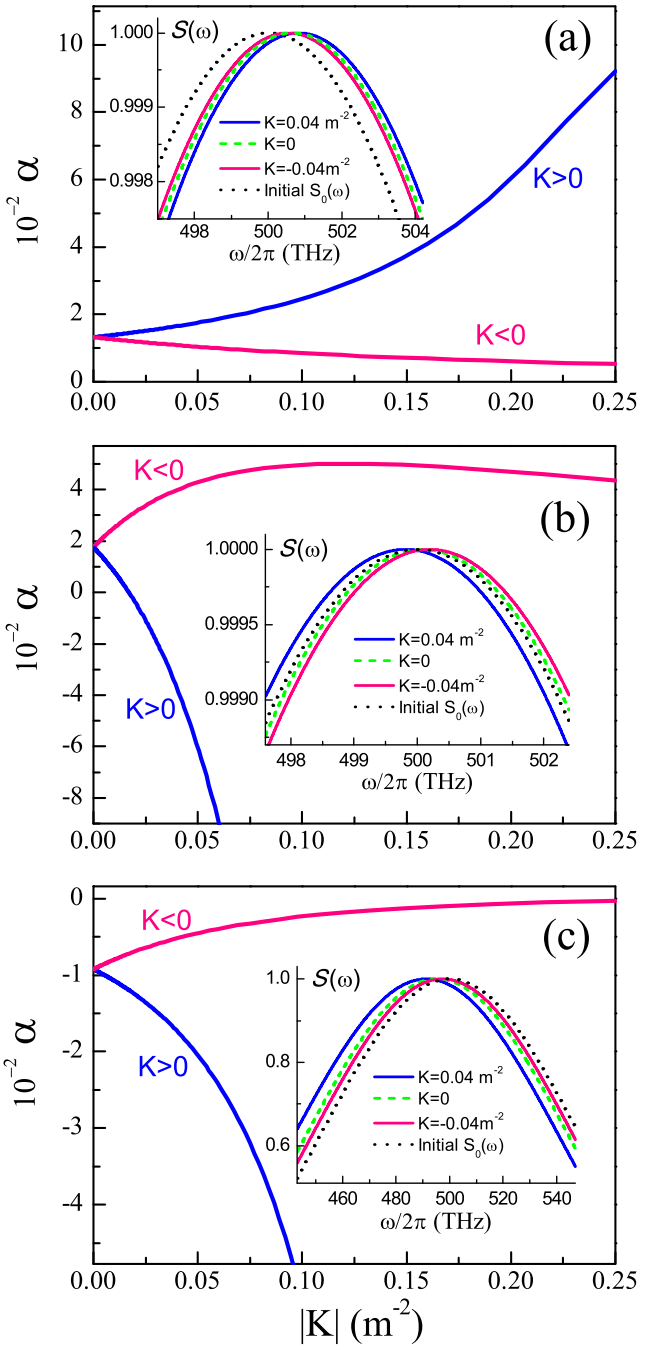


FIG. 2. Typical effect of curvature $K$ on the relative spectral shift $\alpha$ on such 2D surfaces of revolution at different transverse observation positions: (a) $x = 0$, (b) $x = 1$ mm, and (c) $x = 3$ mm, with $z = 3$ m. Here different cases with positive and negative curvature are indicated by the red and blue solid lines, respectively. The insets in (a)–(c) show the normalized output light spectra $S(\omega)$ at the corresponding observation points for the curvature $K = 0.04\text{m}^{-2}$, $-0.04$ m$^{-2}$, in comparison with the initial spectrum and the case of free space ($K = 0$). Other parameters in the calculations are $\omega_0/2\pi = 500$ THz, $\delta/\omega_0 = 0.1$, $\sigma_s = 1$ mm, $\sigma_g = 0.5$ mm, and $n_{\text{eff}} = 1.51$.

where $S_0'$ and $\Omega_q'$, respectively, denote the derivatives of the functions $S_0$ and $\Omega_q$ over frequencies at $\omega_1$. From Eq. (10), it is clear that the spectral shifts are mainly affected by the factor $\Omega_q(z,\omega)$ and they are also influenced by transverse coordinate

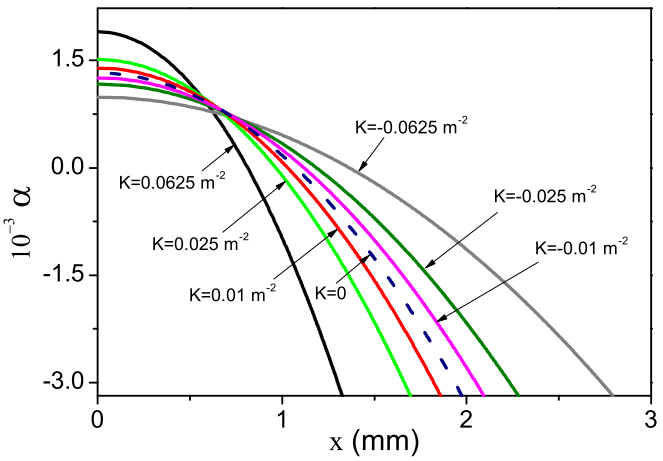


FIG. 3. Typical behaviors of the relative spectral shifts of light along the transverse direction on 2D surfaces of revolution under different values of curvature. Here we take $K = \pm 0.0625$, $\pm 0.025$, and $\pm 0.01 \mathrm{m}^{-2}$, with $z = 3$ m. For comparison, the case of flat space ($K = 0$) is also plotted by the dashed line. Other parameters in the calculations are the same as those in Fig. 2.

values $x$. Since $\Omega_q(z,\omega)$ contains the influence of the curvatures of curved surfaces, the spectral shifts strongly depend on the value of $K$. In a special case, when $\omega_1 = \omega_0$, i.e., there is no spectral shift, then Eq. (10) can be simplified to

$$x = \pm \sigma_s \Omega_q(z,\omega_0). \tag{11}$$

In the above, we have already used the property of $S_0'(\omega_0) = 0$. Clearly the zero spectral shift happens along the change of beam width at the center frequency. In mathematics, since $\Omega_q(z,\omega)$ decreases as frequency increases, also see Eq. (7), $\Omega_q'(z,\omega_1)$ is always negative. Meanwhile both $S_0(\omega_1)$ and $\Omega_q(z,\omega_1)$ are always positive, and $S_0'(\omega_1) > 0$ when $\omega_1 < \omega_0$ and $S_0'(\omega_1) < 0$ when $\omega_1 > \omega_0$. Therefore, from Eq. (10), it is known that in the region of $|x| < \sigma_s \Omega_q(z,\omega_0)$, only the blueshifts are possible; while in the region of $|x| > \sigma_s \Omega_q(z,\omega_0)$, there only exist the redshifts. Interestingly, on the propagating axis (i.e., $x = 0$), from Eq. (10), it can be simplified into $S_0'(\omega_1)/S_0(\omega_1) = \Omega_q'(z,\omega_1)/\Omega_q(z,\omega_1) < 0$, which indicates the blueshift effect. For a single Gaussian spectral line like Eq. (9), the peak frequency $\omega_1$ of the resulting spectrum satisfies a quartic equation: $B\omega_1^4 - B\omega_0\omega_1^3 + \omega_1^2 - \omega_0\omega_1 - \delta^2 = 0$, where the constant $B = (4n_{\mathrm{eff}}^2\sigma_s^4\sigma_g^2)/[c^2R^2\tan_q^2(z/R)(\sigma_g^2 + 4\sigma_s^2)]$ depends on both the parameters (such as the coherence width and beam width) of the light source and the curvatures of the curved surfaces. Our numerical calculations show that only one root of this quartic equation is a real and positive value under the above condition.

Figure 4 clearly demonstrates the distributions of the relative spectral shifts under different situations with different coherence. In all these cases, when the observation point is close to the propagating axis $z$, the resulting spectrum always moves to the higher frequency; while it moves to the lower frequency when the observation point is far away from the propagating axis $z$. In the cases of $K > 0$, when the light source has good coherence with a large value of $\sigma_g$, it is seen that the blueshift range reduces as the propagating distance increases [see Fig. 4(a1)]. This effect is due to the oscillation term contained in Eq. (7), which can be rewritten as

$$\Omega_{+1}(z,\omega) = \left\{1 + \left[\frac{R^2}{Z_R^2(\omega)} - 1\right]\sin^2(z/R)\right\}^{1/2} \tag{12}$$

for $K > 0$. From Eqs. (11) and (12), the blueshift range shrinks under the condition of $R^2 < Z_{R0}^2 \equiv Z_R^2(\omega_0)$, where $Z_{R0}$ is the Rayleigh distance of such partially coherent polychromatic light beams at the center frequency. That is to say, when $K > 1/Z_{R0}^2$, the blueshift range never exceeds the range of $(-\sigma_s,\sigma_s)$ in the transverse direction, and it can even reduce because of the negative coefficient $(R^2/Z_{R0}^2 - 1)$ in the front of the factor $\sin^2(z/R)$. For partially coherent light, the smaller the value of $\sigma_g$, the smaller the values of both $Z_{R0}$ and $Z_R(\omega)$. Thus for a fixed value $R$ (or $K$), both $R^2 = Z_{R0}^2$ and $R^2 > Z_{R0}^2$ may also happen when $\sigma_g$ decreases. Figures 4(a2) and 4(a3), respectively, plot the other two different situations. It is clear that the blueshift range does not change under the critical condition for $R^2 = Z_{R0}^2$, which corresponds to the critical value of the coherence width $\sigma_{g,c} = 2\sigma_s R/(4k_{\mathrm{eff},0}^2\sigma_s^4 - R^2)^{1/2}$, where $k_{\mathrm{eff},0} = \omega_0 n_{\mathrm{eff}}/c$ is the effective wave number at the center frequency. In this example, $\sigma_{g,c} \approx 0.255$ mm. When $R^2 > Z_{R0}^2$, the blueshift range increases as the propagating distance $z$ increases [see Fig. 4(a3)]. One should also notice that when $R^2 > 4k_{\mathrm{eff},0}^2\sigma_s^4$, $\sigma_{g,c}$ does not exist, therefore in this situation the typical spectral shifts in such curved surfaces with $K > 0$ have the same behavior similar to the result in Fig. 4(a3). From Figs. 4(a1)–4(a3), it is found that although the curvature of the curved space is fixed, the spectral changes in the curved space are affected by different values of $\sigma_g$, i.e., the correlation property of the light source. Such spectral changes in Figs. 4(a1)–4(a3) also provide the possibility to determine the curvature of the curved space.

Different from the results in the cases of $K > 0$, the blueshift range always increases with the propagating distance $z$ in the curved space of $K < 0$ [see Figs. 4(c1)–4(c3)]. Meanwhile, it should also be noticed that in the curved space of $K < 0$, the blueshift range increases much quickly with a decrease in the value of coherence width $\sigma_g$. Compared with the cases in the flat space with $K = 0$ [see Figs. 4(b1)–4(b3) and Figs. 4(d1)–4(d3)], in each corresponding case of $\sigma_g$, the positions of zero-spectral shifts in the cases of $K > 0$ are always smaller than those in $K = 0$; but the positions of zero-spectral shifts in the cases of $K < 0$ are always larger than those in $K = 0$. These properties further demonstrate that under the same condition of $\sigma_g$, the spectral shifts are accelerated to the blue- or redshifts due to the curved surfaces with $K > 0$, and they are decelerated to the blue- or redshifts due to the surfaces with $K < 0$. Lastly, it should be emphasized that in the limit of an incoherent light ($\sigma_g \to 0$), since the value of $\Omega_q(z,\omega)$ goes to infinity, ideally the blueshift phenomenon always occurs for any finite transverse coordinate $x$ at $z > 0$. The limit value of the blueshift is given by $\alpha \approx \delta^2/\omega_0^2$ for a single Gaussian spectrum.

## V. CONCLUSION

We have investigated the Wolf effect of a partially coherent polychromatic light beam on the 2D curved surfaces of

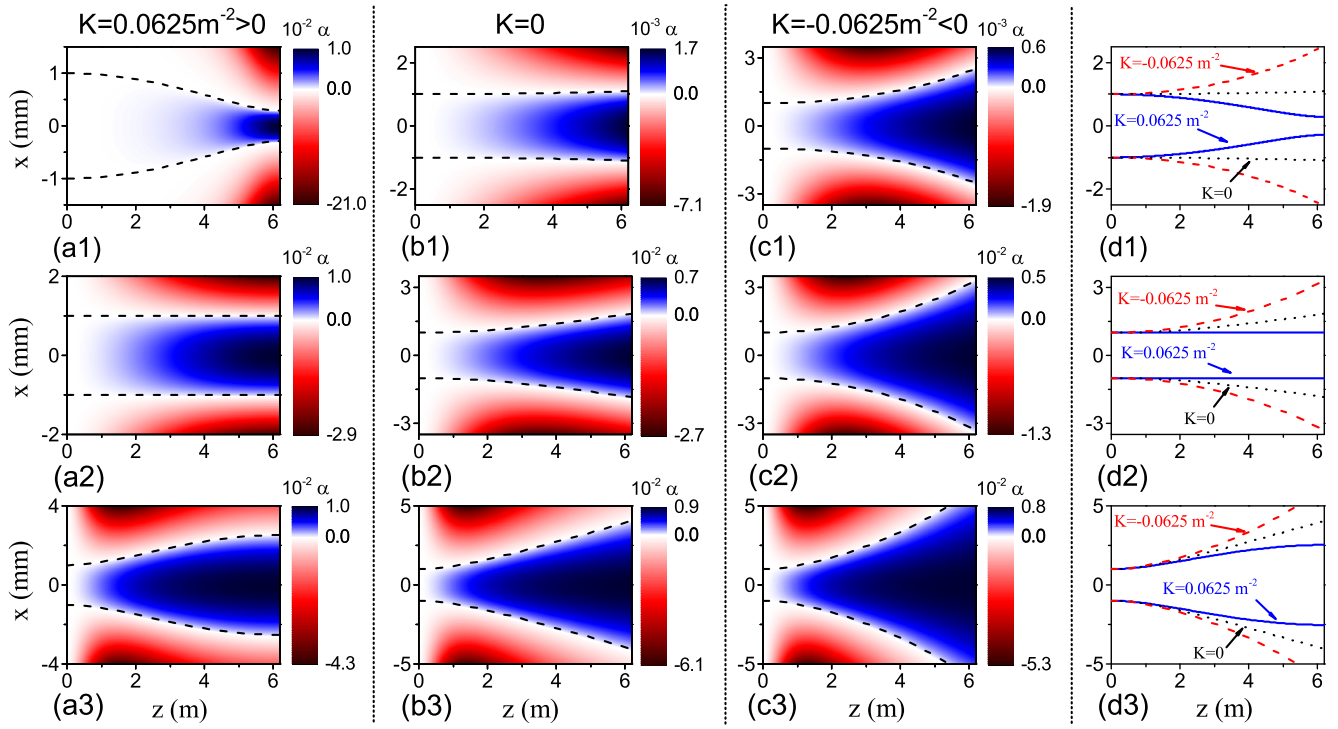


FIG. 4. Distributions of relative spectral shifts on such 2D surfaces of revolution with positive (a1)–(a3) and negative (c1)–(c3) curvature under different correlation lengths $\sigma_g$. For comparison, the corresponding distributions of relative spectral shifts in 2D flat space ($K = 0$) are also shown in (b1)–(b3). The black dashed lines in each case denote the trajectories for zero spectral shifts, see Eq. (11). For a better comparison, the trajectory curves for no spectral shifts in columns (a)–(c) for different $\sigma_g$ are plotted together in (d1)–(d3), respectively. The parameters of the curved spaces are (a1)–(a3) $K = 0.0625\ \mathrm{m}^{-2}$ and (c1)–(c3) $K = -0.0625\ \mathrm{m}^{-2}$, and the values of $\sigma_g$ are (a1), (b1), (c1), (d1) $\sigma_g = 1$ mm; (a2), (b2), (c2), (d2) $\sigma_g \approx 0.255$ mm; and (a3), (b3), (c3), (d3) $\sigma_g = 0.1$ mm. Other parameters are the same as those in Fig. 2.

revolution. Under the paraxial approximation, the space curvature has strong influence on both the on-axis blueshifts and off-axis redshifts of light spectra during their propagations in curved spaces. Besides the correlation of source, curvature also gives rise to the red- and blueshift. Compared with the results of the Wolf effect in flat space, these results indicate that the surfaces with larger positive curvature accelerate the spectral shift to the blue- or redshift along the transverse coordinates, while the spaces with larger negative curvature decelerate and reduce such shifts. By controlling the correlation length of light sources, different evolutions of the Wolf effect are obtained even in the same curved space. This may provide another possible method to probe the curvature of space by measuring the changes in light spectra during their propagation in curved spaces, like the method for measuring the evolution of speckle sizes in curved spaces [57].

## ACKNOWLEDGMENTS

This research is supported by Zhejiang Provincial Natural Science Foundation of China under Grant No. LD18A040001, the National Key Research and Development Program of China (Grant No. 2017YFA0304202), the National Natural Science Foundation of China (Grants No. 11674284 and No. U1330203), and the Fundamental Research Funds for the Center Universities (Grant No. 2017FZA3005). M.S.Z. also acknowledges the support of the NPRP Grant No. 8-751-1-157 from the Qatar National Research Fund.

[1] A. V. Shchegrov, K. Joulain, R. Carminati, and J.-J. Greffet, Near-Field Spectral Effects due to Electromagnetic Surface Excitations, Phys. Rev. Lett. **85**, 1548 (2000).
[2] E. Wolf, Invariance of the Spectrum of Light on Propagation, Phys. Rev. Lett. **56**, 1370 (1986).
[3] E. Wolf, Non-cosmological redshifts of spectral lines, Nature **326**, 363 (1987).
[4] E. Wolf and D. F. V. James, Correlation-induced spectral changes, Rep. Prog. Phys. **59**, 771 (1996).
[5] R. W. Schoonover, B. J. Davis, and P. S. Carney, The generalized wolf shift for cyclostationary fields, Opt. Express **17**, 4705 (2009).
[6] I. Ferreras and I. Trujillo, Testing the wavelength dependence of cosmological redshift down to $\Delta z \sim 10^{-6}$, Astrophys. J. **825**, 115 (2016).
[7] J.-J. Greffet, R. Carminati, K. Joulain, J.-P. Mulet, S. Mainguy, and Y. Chen, Coherent emission of light by thermal sources, Nature **416**, 61 (2002).
[8] G. M. Morris and D. Faklis, Effects of source correlation on the spectrum of light, Opt. Commun. **62**, 5 (1987).

[9] D. Faklis and G. M. Morris, Spectral shifts produced by source correlations, Opt. Lett. **13**, 4 (1988).

[10] M. F. Bocko, D. H. Douglass, and R. S. Knox, Observation of Frequency Shifts of Spectral Lines Due to Source Correlations, Phys. Rev. Lett. **58**, 2649 (1987).

[11] R. W. Schoonover, R. Lavarello, M. L. Oelze, and P. S. Carney, Observation of generalized wolf shifts in short pulse spectroscopy, Appl. Phys. Lett. **98**, 251107 (2011).

[12] H. C. Kandpal, Experimental observation of the phenomenon of spectral switch, J. Opt. A. **3**, 296 (2001).

[13] S. Anand, B. K. Yadav, and H. C. Kandpal, Experimental study of the phenomenon of $1 \times N$ spectral switch due to diffraction of partially coherent light, J. Opt. Soc. Am. A. **19**, 2223 (2002).

[14] R. Zhu, S. Sridharan, K. Tangella, A. Balla, and G. Popescu, Correlation-induced spectral changes in tissues, Opt. Lett. **36**, 4209 (2011).

[15] T. A. Leskova, A. A. Maradudin, A. V. Shchegrov, and E. R. Méndez, Spectral Changes of Light Scattered from a Bounded Medium with a Random Surface, Phys. Rev. Lett. **79**, 1010 (1997).

[16] D. Zhao, O. Korotkova, and E. Wolf, Application of correlation-induced spectral changes to inverse scattering, Opt. Lett. **32**, 3483 (2007).

[17] M. Lahiri and E. Wolf, Relationship between Complete Coherence in the Space-Time and in the Space-Frequency Domains, Phys. Rev. Lett. **105**, 063901 (2010).

[18] M. Amiri, M. T. Tavassoly, H. Dolatkhah, and Z. Alirezaei, Tunable spectral shifts and spectral switches by controllable phase modulation, Opt. Express **18**, 25089 (2010).

[19] T. van Dijk, D. G. Fischer, T. D. Visser, and E. Wolf, Effects of Spatial Coherence on the Angular Distribution of Radiant Intensity Generated by Scattering on a Sphere, Phys. Rev. Lett. **104**, 173902 (2010).

[20] T. Hansson, M. Lisak, and D. Anderson, Integrability and Conservation Laws for the Nonlinear Evolution Equations of Partially Coherent Waves in Noninstantaneous Kerr Media, Phys. Rev. Lett. **108**, 063901 (2012).

[21] C. Sun, L. Waller, D. V. Dylov, and J. W. Fleischer, Spectral Dynamics of Spatially Incoherent Modulation Instability, Phys. Rev. Lett. **108**, 263902 (2012).

[22] L. G. Wang, S. Y. Zhu, and M. S. Zubairy, Goos-Hänchen Shifts of Partially Coherent Light Fields, Phys. Rev. Lett. **111**, 223901 (2013).

[23] J. Svozilík, A. Vallés, J. Peřina, Jr., and J. P. Torres, Revealing Hidden Coherence in Partially Coherent Light, Phys. Rev. Lett. **115**, 220501 (2015).

[24] O. Korotkova, L. Ahad, and T. Setala, Three-dimensional electromagnetic gaussian schell-model sources, Opt. Lett. **42**, 1792 (2017).

[25] W. G. Unruh, Experimental Black-Hole Evaporation? Phys. Rev. Lett. **46**, 1351 (1981).

[26] R. Schützhold and W. G. Unruh, Gravity wave analogues of black holes, Phys. Rev. D **66**, 044019 (2002).

[27] S. Weinfurtner, E. W. Tedford, M. C. J. Penrice, W. G. Unruh, and G. A. Lawrence, Measurement of Stimulated Hawking Emission in an Analogue System, Phys. Rev. Lett. **106**, 021302 (2011).

[28] L. J. Garay, J. R. Anglin, J. I. Cirac, and P. Zoller, Sonic Analog of Gravitational Black Holes in Bose-Einstein Condensates, Phys. Rev. Lett. **85**, 4643 (2000).

[29] C. Barceló, S. Liberati, and M. Visser, Probing semiclassical analog gravity in bose-einstein condensates with widely tunable interactions, Phys. Rev. A **68**, 053613 (2003).

[30] P. O. Fedichev and U. R. Fischer, Gibbons-Hawking Effect in the Sonic de Sitter Space-Time of an Expanding Bose-Einstein-Condensed Gas, Phys. Rev. Lett. **91**, 240407 (2003).

[31] O. Lahav, A. Itah, A. Blumkin, C. Gordon, S. Rinott, A. Zayats, and J. Steinhauer, Realization of a Sonic Black Hole Analog in a Bose-Einstein Condensate, Phys. Rev. Lett. **105**, 240401 (2010).

[32] U. Leonhardt and P. Piwnicki, Relativistic Effects of Light in Moving Media with Extremely Low Group Velocity, Phys. Rev. Lett. **84**, 822 (2000).

[33] M. Visser, Comment on Relativistic Effects of Light in Moving Media with Extremely Low Group Velocity, Phys. Rev. Lett. **85**, 5252 (2000).

[34] U. Leonhardt and P. Piwnicki, Leonhardt and Piwnicki Reply:, Phys. Rev. Lett. **85**, 5253 (2000).

[35] R. Schützhold, G. Plunien, and G. Soff, Dielectric Black Hole Analogs, Phys. Rev. Lett. **88**, 061101 (2002).

[36] I. I. Smolyaninov, Surface plasmon toy model of a rotating black hole, New J. Phys. **5**, 147 (2003).

[37] R. Schützhold and W. G. Unruh, Hawking Radiation in an Electromagnetic Waveguide? Phys. Rev. Lett. **95**, 031301 (2005).

[38] C. Sheng, R. Bekenstein, H. Liu, S. Zhu, and M. Segev, Wavefront shaping through emulated curved space in waveguide settings, Nat. Commun. **7**, 10747 (2016).

[39] X. Wang, H. Chen, H. Liu, L. Xu, C. Sheng, and S. Zhu, Self-Focusing and the Talbot Effect in Conformal Transformation Optics, Phys. Rev. Lett. **119**, 033902 (2017).

[40] A. Greenleaf, Y. Kurylev, M. Lassas, and G. Uhlmann, Electromagnetic Wormholes and Virtual Magnetic Monopoles from Metamaterials, Phys. Rev. Lett. **99**, 183901 (2007).

[41] T. G. Philbin, C. Kuklewicz, S. Robertson, S. Hill, F. König, and U. Leonhardt, Fiber-optical analog of the event horizon, Science **319**, 1367 (2008).

[42] C. Sheng, H. Liu, Y. Wang, S. N. Zhu, and D. A. Genov, Trapping light by mimicking gravitational lensing, Nat. Photon. **7**, 902 (2013).

[43] R. Bekenstein, R. Schley, M. Mutzafi, C. Rotschild, and M. Segev, Optical simulations of gravitational effects in the newton-schrödinger system, Nat. Phys. **11**, 872 (2015).

[44] T. Roger, C. Maitland, K. Wilson, N. Westerberg, D. Vocke, E. M. Wright, and D. Faccio, Optical analogues of the newton-schrödinger equation and boson star evolution, Nat. Commun. **7**, 13492 (2016).

[45] E. E. Narimanov and A. V. Kildishev, Optical black hole: Broadband omnidirectional light absorber, Appl. Phys. Lett. **95**, 041106 (2009).

[46] D. A. Genov, S. Zhang, and X. Zhang, Mimicking celestial mechanics in metamaterials, Nat. Phys. **5**, 687 (2009).

[47] B. S. DeWitt, Dynamical theory in curved spaces. I. A review of the classical and quantum action principles, Rev. Mod. Phys. **29**, 377 (1957).

[48] R. C. T. da Costa, Quantum mechanics of a constrained particle, Phys. Rev. A **23**, 1982 (1981).

[49] S. Batz and U. Peschel, Linear and nonlinear optics in curved space, Phys. Rev. A **78**, 043821 (2008).

[50] V. H. Schultheiss, S. Batz, A. Szameit, F. Dreisow, S. Nolte, A. Tünnermann, S. Longhi, and U. Peschel, Optics in Curved Space, Phys. Rev. Lett. **105**, 143901 (2010).

[51] S. Batz and U. Peschel, Solitons in curved space of constant curvature, Phys. Rev. A **81**, 053806 (2010).

[52] G. D. Valle and S. Longhi, Geometric potential for plasmon polaritons on curved surfaces, J. Phys. B: At. Mol. Opt. Phys. **43**, 051002 (2010).

[53] R. Bekenstein, J. Nemirovsky, I. Kaminer, and M. Segev, Shape-Preserving Accelerating Electromagnetic Wave Packets in Curved Space, Phys. Rev. X **4**, 011038 (2014).

[54] A. Patsyk, M. A. Bandres, R. Bekenstein, and M. Segev, Observation of Accelerating Wave Packets in Curved Space, Phys. Rev. X **8**, 011001 (2018).

[55] E. Lustig, M.-I. Cohen, R. Bekenstein, G. Harari, M. A. Bandres, and M. Segev, Curved-space topological phases in photonic lattices, Phys. Rev. A **96**, 041804(R) (2017).

[56] R. Spittel, P. Uebel, H. Bartelt, and M. A. Schmidt, Curvature-induced geometric momenta: The origin of waveguide dispersion of surface plasmons on metallic wires, Opt. Express **23**, 12174 (2015).

[57] V. H. Schultheiss, S. Batz, and U. Peschel, Hanbury brown and twiss measurements in curved space, Nat. Photon. **10**, 106 (2016).

[58] C. Conti, Localization and shock waves in curved manifolds, Sci. Bull. **61**, 570 (2016).

[59] K.-B. Hong, C.-Y. Lin, T.-C. Chang, W.-H. Liang, Y.-Y. Lai, C.-M. Wu, Y.-L. Chuang, T.-C. Lu, C. Conti, and R.-K. Lee, Lasing on nonlinear localized waves in curved geometry, Opt. Express **25**, 29068 (2017).

[60] E. R. Harrison, *Cosmology: The Science of the Universe*, 2nd ed. (Cambridge University, New York, 2000).

[61] D. F. V. James, The Wolf Effect and the Redshift of Quasars, Pure Appl. Opt. **7**, 959 (1998).

[62] L. Mandel and E. Wolf, *Optical Coherence and Quantum Optics* (Cambridge University, New York, 1995).

[63] J. T. Foley and M. S. Zubairy, The directionality of Gaussian Schell-model beams, Opt. Commun. **26**, 297 (1978).

[64] G. P. Agrawal and A. Gamliel, Spectrum of partially coherent light: Transition from near to far zone, Opt. Commun. **78**, 1 (1990).